Conference on Fourier Transform Spectroscopy 2001, Coeur d'Alene, ID (Feb 5-8, 2001). Paper PDP2.

Real-time discrimination of spectra by time-domain adaptive filtering in a Fourier transform interferometer

S. R. Bhalotra, H. L. Kung, and D. A. B. Miller
Edward L. Ginzton Laboratory, Stanford University, Stanford, California 94305-4085
sbhalotra@stanford.edu

Abstract: We present a programmable spectral discrimination system with minimal data extraction and processing, insensitive to scan nonlinearities. We demonstrate real-time discrimination of monochromatic sources 30 nm apart, employing a spectrometer with a nominal resolution of 200 nm.

OCIS codes: (300.6300) Spectroscopy, Fourier transforms; (120.6200) Spectrometers and spectroscopic instrumentation

1. Introduction

In recent years there has been a dramatic increase in the generation, transmission, storage, and processing of hyperspectral images in sensing applications [1]. Platforms such as helicopters and vehicles require mobile sensor units with fast analysis of information from compact systems [2]. Here we present a new method of adaptive time-domain processing for real-time discrimination of spectra. We demonstrate a programmable Michelson interferometer system that functions without the need to characterize scan nonlinearities. This method allows very simple spectrometers to perform sophisticated sensing tasks with minimal data processing power. This broadens the field of usable MEMS (Micro-Electro-Mechanical Systems) components for implementation in miniaturized sensing systems [3].

Often sensing system are tasked with distinguishing one spectrum from a set of known spectra. There are many ways to solve this type of problem. One such method is to calculate and compare overlap integrals between the test spectrum and the set of reference spectra. Though this is typically done in the frequency domain, we suggest a system that operates in the time domain. For a discrete set of data, this is an inner product.

This inner product can be computed in many ways. We employ time-domain electronic multiplication followed by electronic integration. Photodetector output representing an optical signal of interest is multiplied by a synchronized reference function. Processing is completed as soon as the interferometer finishes scanning, thus making this a real-time system. Reference functions are acquired by recording the appropriate interference signals from the photodetector with the same system, including the effects of any nonlinearities in the mirror motion. Nonlinearities therefore need not be characterized explicitly and require no data post-processing. This yields considerable freedom to design and implement systems that utilize simple components (e.g., a sinusoidal mirror scan, for example).

This inner product system necessitates gathering much less information to solve the problem of discrimination of spectra. The set of reference functions contains information, thus requiring less from the spectrometer. With *a priori* information about the target spectra, it is possible to discriminate spectra beyond standard Fourier transform resolution limits.

2. Optical and Electronic Systems

The optical set-up is a Michelson interferometer, as shown in Fig. 1. The scanning mirror is a 4 mm square piece of 500 μm thick silicon with a 3500 Å reflective aluminum coating, mounted on a piezoelectric transducer (PZT). The detector is an amplified silicon PIN photodiode, preceded by a 9 cm focusing lens. For the simple discrimination experiment, we use two lasers as the light sources, a HeNe laser at 633 nm with 281 μW power, and a laser diode at 663 nm with 328 μW power. Both have ~ 1.5 mm diameter beams. To maximize source stability, an optical isolator composed of a linear polarizer and quarter wave plate is employed to prevent feedback.

As an example of nonlinear motion, the PZT is driven with a DC-offset sinusoid at 0.1 Hz, by a function generator and high voltage amplifier. The detector output connects directly to electronic circuitry which filters, amplifies, and processes data in real-time. Controlled by computer, the electronics (Fig. 2) can either send measured interference functions to a synchronized data acquisition interface for recording or multiply and integrate the signal with a synchronized reference function, sending only the final inner product value for data acquisition. We use an analog multiplier I.C., MPY634, and an integrator with an op-amp I.C., LF347N.

Fig. 3 illustrates typical filter functions and step-by-step calculation of a set of inner products. AC-coupling of the reference function is critical, as DC components of the multiplied signal should not come from the product of DC-offsets in both signals. This system can be reprogrammed to distinguish between different spectral sets simply by recording and storing a new set of reference functions.

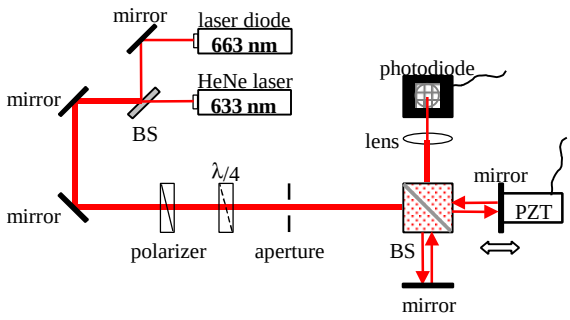

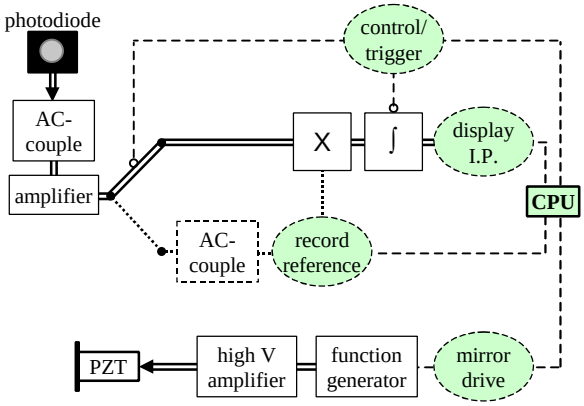

Fig. 1 (left). Optical set-up. Two lasers are coupled into a Michelson interferometer via a beamsplitter (BS) and an isolator.

Fig. 2 (right). System electronics. Photocurrent from the interferometer is either recorded as a reference function or routed to the inner product (I.P.) stages in real-time. The CPU controls these operations as well as the scanning mirror drive parameters.

3. Inner Product Theory

The reference functions can be calculated theoretically by combining the standard sinusoidal interference function with the mirror drive function. Eq. 1 shows the interference photocurrent I as a function of mirror position z, for maximum photocurrent A, source wavelength λ, and mirror scan length d. Eq. 2 shows the mirror position z as a function of time t, where f is the frequency of mirror oscillation.

$$I[z] = \frac{A}{2}\left[1+\cos\left(\frac{4\pi}{\lambda}z\right)\right],\ z\in[0,d] \qquad z[t] = \frac{d}{2}\left[1-\cos(2\pi ft)\right],\ t\in\left[0,\frac{1}{2f}\right] \qquad (1,2)$$

It is necessary to take into account the absolute phase difference ε at the detector between the test function and the reference function, as well as the exact location of the mirror starting point for each scan. The absolute starting point is generally different for different scan lengths. The PZT moves around the position determined by the DC offset of the drive voltage signal, so the scan endpoints in free space are determined by the AC voltage applied, which depends on the maximum displacement desired. Thus the starting point for each mirror scan depends on the scan length, which implies a variable relative starting phase between each wavelength. This can be well approximated to first order by an added wavelength-dependent phase shift offset $\theta = 4\pi Bd/\lambda$ at the start of each scan, where B is a scaling constant dependent on the PZT's response characteristics. Eq. 3 shows the complete theoretical reference function, AC-coupled from the photodetector output.

$$I[t] = \frac{A}{2}\left[\cos\left(\frac{2\pi d}{\lambda}\left\{1-\cos(2\pi t)\right\}+\varepsilon+B\frac{4\pi d}{\lambda}\right)\right],\ t\in\left[0,\frac{1}{2f}\right] \qquad (3)$$

With the 633 nm source coupled into the interferometer, theoretical inner products with 633 nm and 663 nm reference functions are plotted as thin solid lines in Fig. 4. The upper curve, representing the magnitude of the 633 nm interference function, is flat on average. The lower curve is separated from the upper at high mirror scan lengths, and the separation generally decreases with scan length. Where the upper inner product is greater than the lower, discrimination is straightforward. This calculation yields a small, high frequency oscillatory term at four times the 633 nm light frequency on the upper curve and two times the sum of the 633 nm and 663 nm frequencies on the lower curve. The small, lower frequency oscillation on both curves is due to the θ term. The large, low frequency oscillation on the lower curve, which has the most important effect on discrimination, is essentially two times the difference between the 633 nm and 663 nm light frequencies, adjusted by the θ term.

All oscillations on both curves are larger at lower mirror scan lengths. Since the number of data points acquired for recorded functions is only dependent on scan time, which is constant for a fixed mirror drive frequency, there is implicit normalization of the inner product by mirror scan length. Sinusoidal mirror motion augments this effect.

Since the mirror slows down at the ends of its scan, the inner product weights the ends of the scan more heavily. At lower scan lengths, where the end regions are a high fraction of the total function, the oscillations are larger.

The rapid decrease of the theoretical inner product curves below 1.0 μm scan length is due to precision digital AC-coupling of the reference functions when recording. When functions with few fringes are AC-coupled, they can be significantly offset, causing degeneration of the inner product.

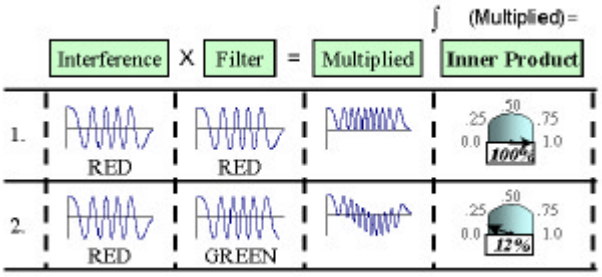

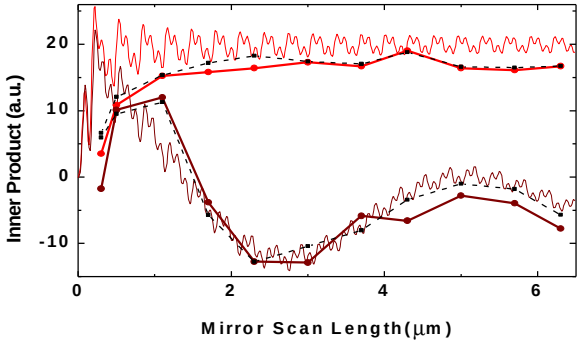

Fig. 3 (left). Graphical explanation of inner product. Two theoretical interference functions are multiplied and integrated, demonstrating a large difference that could be used to discriminate them.

Fig. 4 (right). Inner products (I.P.). Upper curves represent I.P. of 633 nm signal with 633 nm reference. Lower curves are I.P. of same signal with 663 nm reference. Thin solid lines represent theoretical simulations; dashed lines are digital calculations with recorded reference functions; thick solid lines are electronic I.P. calculated in real-time.

4. Experimental Results

Experimental inner products, recorded in real-time and measured for a series of mirror scan lengths 0.66 μm apart, are also plotted in Fig. 4. Mirror scan length, which is total peak-to-peak mirror displacement, is measured by analyzing the interference signal from a known monochromatic source. Real-time data follows theory, except for a decline steeper than expected at very low scan lengths. This is due to relative instability of the PZT motion in this regime, which dilutes the inner product. The dashed lines represent inner products calculated digitally from recorded reference functions. They are very similar to the curves calculated in electronics, thus there is no significant discrimination disadvantage of real-time inner products. The majority of deviation from the theory is due to differences between the actual interference functions recorded and the theoretically generated functions.

It is possible to discriminate the two sources here at mirror scan lengths significantly lower than those suggested by the spectrometer system's resolution. For discriminating 633 nm and 663 nm wavelengths, standard resolution criteria suggest a scan length of 7.0 μm. Our system reports the correct source with greater than 90% accuracy at a scan length of 1 μm. This advantage decreases required PZT driver output current and power, frequency response of detectors and electronics, and maximum displacement and size of mirror actuator. This spectrometer, with a scan length of 1 μm, implying a conventional resolution of ~ 200 nm, can reliably discriminate light sources only 30 nm apart in wavelength.

5. Conclusion

This method of time-domain filtering expands the possibilities for design of simple, compact, adaptive spectrometers. Insensitivity to nonlinear scanning can accommodate many types of MEMS devices, and reduction in required mirror displacement can dramatically relax operating requirements on the system. Inherent programmability and extraction of minimal data, in comparison with a large data set needed for an accurate full spectral analysis, bring speed and flexibility. Time-domain calculation and the lack of computer-intensive processing can aid the design of fast, mobile sensing systems.

6. References

[1] N. Gat, "Imaging spectroscopy using tunable filters: a review," in Wavelet Applications VII, Proc. SPIE 4056, 50-64 (2000).
[2] S. D. Brown, "Real-time filtering of data from mobile passive remote infrared-sensors with principal components models of background," J. of Chemometrics **5**, 147-161 (1991).
[3] H. L. Kung, S. R. Bhalotra, J. D. Mansell, and D. A. B. Miller, "Compact transform spectrometer based on sampling a standing wave," in 2000 Int'l Conference on Optical MEMS, IEEE/LEOS, 19-20 (2000).